Characterization of Film Formation from Polystyrene Latex Particles via SANS. 2. High Molecular Weight

J. N. Yoo,[†,‡,§] L. H. Sperling,[*,†,‡,§,∥,⊥] C. J. Glinka,[¶] and A. Klein[†,§,⊥]

Center for Polymer Science and Engineering, Materials Research Center, Department of Chemical Engineering, Department of Materials Science and Engineering, and Emulsion Polymer Institute, Whitaker Laboratory No. 5, Lehigh University, Bethlehem, Pennsylvania 18015, and Institute for Materials Science and Engineering, National Institute of Standards and Technology, Gaithersburg, Maryland 20899

Received February 16, 1990; Revised Manuscript Received December 12, 1990

ABSTRACT: The interdiffusion of polymer chains during film formation from high molecular weight ($M_w \simeq 2\,000\,000$) polystyrene latex particles of about 270-Å radius was characterized by small-angle neutron scattering (SANS) and correlated with the development of tensile strength of the resulting films. After an apparent induction period, tensile strength increases with annealing time. Full tensile strength was achieved at a penetration depth of 30–35 Å, comparable to the radius of gyration of the critical entanglement molecular weight of polystyrene (32 000 g/mol). Two critical parameters in the interdiffusion process of film formation from latex particles are proposed: the location of chain ends and the dimensionless ratio of the polymer chain's radii of gyration to the latex particle's radius.

Introduction

Until recently, the interdiffusion problem in latex film formation could not be tackled, due to the lack of proper experimental methods. For the first time, using small-angle neutron scattering (SANS), Hahn and co-workers[1,2] reported that coalescence of *n*-butyl methacrylate based copolymer latex particles was due to a massive interdiffusion of polymer chains between particles. Subsequently, Linné et al.[3] observed interdiffusion in film formation from polystyrene latex via SANS, evidenced by an increase in the radius of gyration of polystyrene chains that were initially constrained in small-size latex particles.

Then, critical questions that should be asked include the following: (1) How far must the polymer chains inside the latex particles interdiffuse across the particle boundaries to achieve full film strength? (2) What are the important parameters in the interdiffusion process of polymer chains during film formation from latexes?

The above questions are also raised in the area of interface healing. Latex film formation can be considered as a special case of the interface healing problem such as crack healing and polymer welding. In both cases, strength development is dependent on polymer chain interdiffusion requirements. Considerable progress has been made in understanding the interface healing behavior of polymer systems, and several theories have been proposed[4–10] based upon de Gennes' reptation diffusion model.[11] These theories, while different in detail, commonly assume that the formation of entanglements between polymer chains across the interface is directly responsible for the development of material strength. One of the major conclusions is that fracture stress should increase with healing time to the one-fourth power. Furthermore, the concentration profiles for the chain segment at the interface have been derived.[12,13]

On the other hand, a large number of experimental studies on the interface healing problem have been reported,[3,14–18] some emphasizing the crack healing of crosslinked copolymers of styrene and acrylonitrile,[19] autohesion of branched polybutadiene,[20] and self-adhesion of polyimide having nonrandom polymer chain conformation.[21] In the present paper, attention will be paid to the interface healing of the linear polymer systems from latex particles.

It has been confirmed that an interface gains strength with healing time to the one-fourth power in the crack healing[16] and polymer welding[18] of linear random coil systems such as poly(methyl methacrylate) and polystyrene. Under the specified experimental conditions, the times required for complete healing were also reported,[16,18] from which the minimum interdiffusion penetration depth for full material strength was calculated by using diffusion coefficients of the polymers.[16]

However, the actual interdiffusion penetration depth had not been measured under the same experimental conditions as in the healing experiments until Linné et al.[3] showed that a penetration depth of 50–60 Å across the latex particle boundaries was sufficient to develop fully healed films of polystyrene. This was based on SANS experiments and preliminary indentation toughness tests. Meanwhile, Brown et al.[21] correlated the actual depth of penetration (measured by forward recoil spectrometry) and the adhesion characterized by peel tests using an aromatic polyimide, noting that their interface healing accompanied a chemical reaction. It was found that a penetration depth of at least 2000 Å was required to recover complete strength.

Most recently, we[22,23] have investigated the relationship between the actual depth of penetration and the tensile strength buildup in latex film formation using low molecular weight polystyrene (250 000 g/mol) through the SANS study. The system is unique in that the small-diameter latex particles (550 Å) provided a huge interfacial area for the healing process. The minimum penetration depth for fully developed tensile strength was comparable to the radius of gyration of the polymer chains, and an elbow in the tensile strength–penetration depth plot was observed at the diffusion depth corresponding to the radius of gyration of polystyrene (45–50 Å) of critical entanglement molecular weight (32 000 g/mol).

It is interesting to note that almost all of the linear polymer materials used in the interface healing experiments have been of rather low to moderate (below M_w = 300 000) molecular weights. As pointed out by Tirrell in his excellent review paper on polymer self-diffusion,[24] the

* To whom correspondence should be addressed.
† Center for Polymer Science and Engineering.
‡ Materials Research Center.
§ Department of Chemical Engineering.
∥ Department of Materials Science and Engineering.
⊥ Emulsion Polymer Institute.
¶ Institute for Materials Science and Engineering.

0024-9297/91/2224-2868$02.50/0

evaluation of molecular weight dependence on the development of healing strength has never been made, although the molecular weight dependence of the diffusion coefficient is well established both theoretically[11] and experimentally.[25-27]

As a molecular-level feature of the healing problem, the role of the location of chain ends in the interface healing has been discussed[4-6,10,28] in the past. Apparently, when polymer chain ends are located at the healing interface the recovery of material strength is the fastest as discussed in the crack healing area.[10,11,15,16] However, experimental verification is quite rare, supposedly because of limitations in controlling the location of chain ends. In this regard, latex synthesis renders a way of relieving this limitation, because it has been well-known that persulfate-initiated polystyrene latexes have their chain ends anchored on the particle surfaces.[29-33]

In this paper, to answer the questions raised previously, the relationship between the interdiffusion penetration depth in film formation from very high molecular weight polystyrene latex particles and strength buildup was studied by SANS. The results were compared with those of the previously reported low molecular weight experiments.[22] Using a qualitative model, we will interpret the current data along with the data published to date in the area of interface healing. Emphasis is placed upon the roles of the location of chain ends and the dimensional ratio of polymer chains to the latex particle in the interdiffusion processes during film formation.

Theoretical Background

For the past years, extensive research has been carried out on the subject of polymer interface healing. Based on de Gennes' reptation theory,[11] considerable progress has been made in understanding the interface healing characteristics of polymer systems theoretically.[4-10,12,13,28] It is noted that four theoretical models have been proposed to describe the time and molecular weight dependence of strength development during the course of interface healing. They commonly assume that the formation of entanglements between polymer chains across the interface is essential to recover mechanical strength of the polymer system to be healed. These four models will be briefly compared, emphasizing the differences in the results and assumptions used therein.

(a) de Gennes' Model.[28] In this model, it was assumed that the fracture energy, G_{IC}, is proportional to the number of bridges across the interface. It is reported that G_{IC} increases with the square root of time, and the fracture stress, K_{IC}, increases with time to the one-fourth power.

(b) Prager and Tirrell's Model.[7] This model predicts the number of bridges per unit area spanning the original junction interface as a function of time, t, and the molecular weight, M, of the chains. It was reported that

$$K_{IC} \propto t^{1/4}M^{-3/4} \quad (1)$$

when the inital contact is between surfaces that have been equilibrated against a gas phase. Alternatively, it was also reported that

$$K_{IC} \propto t^{1/8}M^{-1/8} \quad (2)$$

when the contacting surfaces contain many chain ends at short times.

(c) Jud, Kausch, and Williams' Model.[10] It was assumed that interface strength is proportional to the contact surface area ratio A and A_0, where A is the contact area and A_0 is the total cross-sectional area of the interfacial bond, and the proportion of the links formed across that area, N/N_0, where N is the number of links formed across the bond and N_0 is the concentration of links at full strength. Finally, the number of physical links is assumed to be proportional to the average depth of penetration of polymer chains. This model yielded the following relationship:

$$K_{IC} \propto t^{1/4} \quad (3)$$

(d) Minor Chain Reptation Model by Kim and Wool.[5] According to the reptation theory, the constraints imposed on a chain by the entanglements of chains effectively confine a chain inside an imaginary tubelike region. The portions of a chain that are no longer in the initial tube increase with time and are referred to as minor chains in this model. This theory analyzes the motion of the minor chains at the interface and calculates the average interpenetration distance of polymer segments, which was assumed to be proportional to fracture stress, as a function of time and molecular weight. It was also assumed that the distribution of chain ends in the system is uniform. One of the major conclusions is that

$$K_{IC} \propto t^{1/4}M^{-1/4} \quad (4)$$

At least, there is an agreement among these models that during the course of interface healing, strength should increase with time to the one-fourth power, although controversial results were reported on the molecular weight dependence of the healing rate. The time dependence has been confirmed experimentally.[4,10,18] By extension of their theories, Tirrell and co-workers and Wool and coworkers[12,13] derived the concentration profile of polymer segments at the interface.

Data Analysis

The interdiffusion of polymer chains among latex particles was characterized by probing the increase in the apparent size of the deuterated polystyrene latex particles during the course of annealing. As in the previous paper,[22] the well-known Guinier approximation[36] was adopted in the analysis of the SANS data to evaluate the size of the deuterated polystyrene particles. The Guinier approximation at very low angle can be written as

$$\frac{d\Sigma}{d\Omega}(K) = \frac{d\Sigma}{d\Omega}(0)\exp(-K^2R_g^2/3) \quad (5)$$

where $d\Sigma/d\Omega$ is the coherent scattering cross section per unit volume of the material. The quantity K is the scattering vector and R_g represents the radius of gyration.

From the slope of the Guinier plot, which plots logarithmic intensity vs squared scattering vector, in the very low angle region the radius of gyration (R_g) of the deuterated polystyrene particle was determined. For a sphere, the radius, R, is related to the radius of gyration by

$$R^2 = (5/3)R_g^2 \quad (6)$$

Accordingly, the radius of the deuterated polystyrene particles was calculated with the above relationship. The size of the deuterated polystyrene particles, which grow via interdiffusion of polymer chains among neighboring particles, determined by this procedure is an apparent and averaged quantity, because there may be concentration fluctuations of the deuterated polystyrene chain segment at the diffusion front and the expanding deuterated polystyrene particles are not perfect spheres. The model here may be linked to that of an exploding star.

The penetration depth, $d(t)$, of polymer chains across particle boundaries was obtained by subtracting the

original radius, R_0, of the deuterated latex particles in the aqueous dispersions from the radius, $R(t)$, of the expanding deuterated polystyrene particles:

$$d(t) = R(t) - R_0 \tag{7}$$

where t stands for annealing time.

Binder[37] derived an equation to obtain the diffusion coefficient, based on Cook's scattering equation[38] for spinodal decomposition of metal alloys. For the case of an ideal polymer solution, Binder's equation can be written as

$$I(K,t) = I(K,0)\exp(-2K^2Dt) + I(K,\infty)[1 - \exp(-2K^2Dt)] \tag{8}$$

where $I(K,0)$ and $I(K,\infty)$ are the initial and equilibrium scattering intensities, respectively. D is the diffusion coefficient, and t stands for time.

Recently, Summerfield and Ullman[39] derived an equation to obtain the diffusion coefficient from SANS data on systems composed of randomly mixed clusters of protonated and deuterated polymers where Fick's law applies. They showed that $I(K,t)$, the SANS intensity at annealing time t, can be characterized by

$$I(K,t) = I(K,0)\exp(-2K^2Dt) + I(K,\infty)\left[1 - \alpha(0,t) - \frac{1-\beta}{1-\psi}\exp(-2K^2Dt)\right] \tag{9}$$

where $\alpha(0,t)$ is the normalized integral of a radial correlation function, $\alpha(R,0)$, characterizing the initial configurations of the segregated clusters.

$$\alpha(0,t) = (8\pi Dt)^{-3/2}\int_0^\infty \alpha(R,0)\exp(-R^2/8DT)\,dR \tag{10}$$

where R is a radial position. Furthermore, β and ψ are defined by the relationship

$$\alpha(0,0) = \frac{\beta - \psi}{1 - \psi} \tag{11}$$

where $\psi \le \beta \le 1$.

In the current SANS data, $I(K,\infty)$ is much smaller (<10%) than $I(K,0)$, especially in the low angles and short annealing times. Equations 8 and 9 are reduced to the same forms when the second term in eqs 8 and 9 is neglected. On the basis of these equations, a diffusion coefficient can be determined from the slope of the plot, $\ln [I(K,t)/I(K,0)]$ vs K^2t.

Anderson and Jou[40] prepared artificial latexes by a dispersion technique. They used anionically polymerized polystyrene of very narrow molecular weight distribution, but the particles were thought to be both large and polydisperse. The objective of the experiment was to measure the diffusion coefficient of polystyrene using the Summerfield and Ullman theory rather than determine the relationship between interpenetration depth and mechanical behavior. For polystyrene of 68000 g/mol at 130 °C, the diffusion coefficient was found to be of the order of 1×10^{-15} cm^2/s.

Experimental Section

The most desired compositions of matter for the planned experiments would be uniform latexes bearing monodisperse polymer. However, both conditions are difficult to achieve simultaneously at this time. The Anderson and Jou[40] experiments utilized monodisperse molecular weights; however, as mentioned above, their particle sizes were large, and the distribution in sizes was unsatisfactory for the planned experiments. The present experiments will utilize the opposite condition, that of small, uniform particle sizes, bringing with it a broad molecular weight distribution. The following will delineate the preparation procedures.

Table I
Polymerization Recipe of High Molecular Weight Polystyrene Latexes[a]

ingredients	parts by weight
water (deionized distilled)	324.0
styrene	16.0
potassium persulfate	0.9
KOH	0.135
sodium lauryl sulfate (SLS)	0.54
Triton X-100	5.4

[a] Polymerization temperature, 60 °C; reaction time, 22 h.

Table II
Characterization of High Molecular Weight Polystyrene Latexes

sample	M_n	M_w	M_w/M_n	particle radii,[a] Å
deuterated polystyrene	281 000	2 080 000	7.4	266
protonated polystyrene	260 000	1 820 000	7.0	275

[a] Determined by photon correlation spectroscopy.

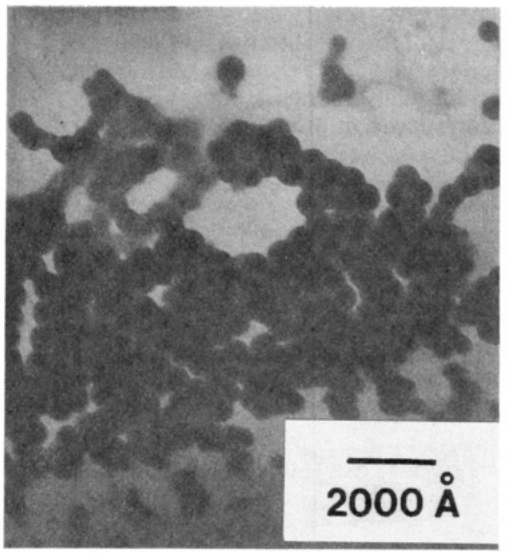

Figure 1. Transmission electron micrograph for the deuterated polystyrene latex particles (magnification: ×72 000).

The experimental conditions employed were identical with those of previous experiments with low molecular weight (M_w = 250 000) polystyrene latexes. Detailed experimental procedures were described in the former paper.[22] The current experiments were performed on very high molecular weight polystyrene latexes.

Specimen Preparation. In the present experiments, very high molecular weight polystyrene latexes were prepared, while maintaining the same particle size of the moderate molecular weight latexes, by using the same recipe excluding the chain-transfer agent, carbon tetrachloride (see Table I). This recipe results in a narrow particle size distribution. Protonated and deuterated polystyrene latexes were synthesized, separately, using batch, bottle emulsion polymerization techniques.

The particle size of the latexes in aqueous dispersion was characterized by photon correlation spectroscopy (Coulter N4MD). A particle size dispersity index of about 1.08 was obtained for both latexes by transmission electron microscopy (Philips 300); see Figure 1. Waters gel permeation chromatography was employed to determine the molecular weight and molecular weight distribution; see Table II.

These two latexes were mixed to give 6 mol % of deuterated polystyrene. The mixed latex was then dried at 40 °C and extracted with excess methanol followed by hot-water extraction

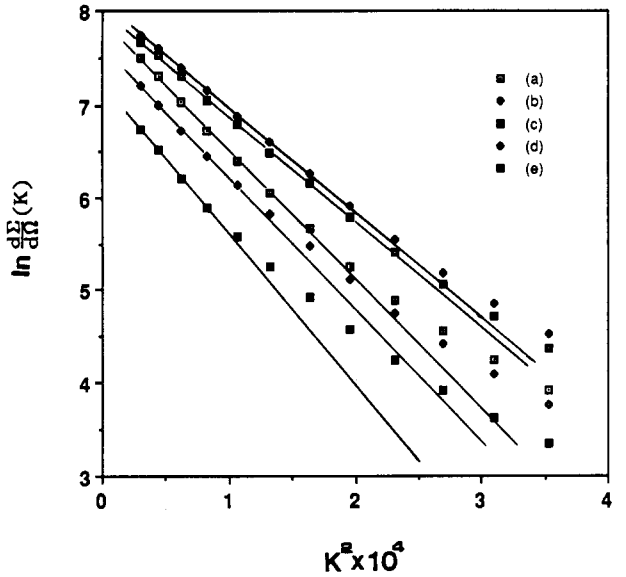

Figure 2. Guinier plots of selected high molecular weight samples: (a) sintered and also annealing times (b) 15 min, (c) 1 h, (d) 19 h, and (e) 48 h at 144 °C.

to remove the surfactants. The resulting wet cake was dried at 60 °C in a vacuum oven. Fourier transform infrared spectroscopy and differential scanning calorimetry showed that almost all of the surfactants were removed. Using a vacuum hot press, sintering of the polystyrene powder was carried out at 110 °C for 40 min under a pressure of 9.0 MPa to yield disk-shaped specimens of about 0.8-mm thickness and 3.75-cm diameter.

The polystyrene films were annealed at 144 °C for various times using the assembly of the previous experiment[22] in a forced convection oven. For each specimen, 30 min of temperature equilibration was allowed before annealing time was initiated.

Following the same procedures described above, 100% protonated specimens for the SANS blank samples as well as for the tensile strength tests were prepared. The results of density measurements by flotation in aqueous NaCl solutions for the three kinds of specimens (SANS, SANS blank, and tensile strength) provided evidence that they were fully dense (density of SANS samples = 1.062 ± 0.004 g/cm³ and density of SANS blanks and tensile specimens = 1.058 ± 0.004 g/cm³).

SANS and Tensile Strength Measurements. The SANS measurements were carried out at two locations, the National Institute of Standards and Technology (NIST) and the Los Alamos Neutron Scattering Center (LANSCE), under the same conditions as the previous experiments,[22] including instrument configuration, neutron wavelength, neutron flux, calibration, and data reduction. The two instruments are somewhat different in principle but give comparable results.[34,35]

SANS data for the bulk films were obtained over the range of scattering vectors $0.0043 < K < 0.08$ Å^{-1} at the NIST facility. To measure the original size of the deuterated polystyrene latex particles excluding the surfactant layer thickness, SANS measurements were made for the deuterated latex and the corresponding protonated polystyrene latex blank at the LANSCE facility. Subtraction of the blank also corrects for the surfactant layer thickness. Useful data were collected at scattering vectors between 0.0037 and 0.1 Å^{-1}.

An Instron universal testing machine was utilized to characterize the tensile strength of 100% protonated polystyrene films of dumbbell-type microspecimens at room temperature. A grip separation rate of 0.254 cm/min and a grip separation distance of 1.25 cm were applied.

Results

SANS data were collected for each sample and blank at NIST. After correction of the sample scattering for the blank, Guinier plots were prepared. Selected data are shown in Figure 2. Only the linear, low-angle portions of the data were used in the calculations, especially at long annealing times.

Table III
Summary of SANS and Tensile Strength Test Results of High Molecular Weight Polystyrene Latex Based Films

annealing time	R_g,[a] Å	av depth of penetration, Å	tensile strength × 10^5, N/m²
dispersed latex	174		
sintered	209		34
5 min	186	15	52
15 min	186	15	64
30 min	186	15	120
1 h	189	19	226
2 h	195	28	389
4 h	199	32	389
8 h	200	35	371
19 h	207	43	345
48 h	216	55	366

[a] Obtained by Guinier approximation.

Tensile strength data were collected on duplicate specimens (in most cases) as a function of annealing time. The standard deviation was approximately 10% between pairs of measurements. The radii of gyration of the samples and the concomitant average depth of interpenetration are shown together with the tensile strength data in Table III.

As might be predicted, the radius of gyration of deuterated polystyrene particles increases as annealing proceeds. As observed in the experiments on low molecular weight polystyrene,[22] the radius of gyration of the sintered particles is apparently larger than the original size of the deuterated polystyrene latex particles. This is attributed to the anisotropy (oblate spheroids) of the deuterated particles which resulted from the high-pressure sintering process. However, the anisotropy vanishes through physical relaxation on annealing, as evidenced by an increase in specimen thickness and a decrease in specimen diameter after a short period of annealing.[40,41]

Thus, there is no apparent increase in the depth of penetration until after 30 min of annealing time. This is most likely due to the artifact resulting from two competing processes during the early stages of annealing: (1) the recovery of particle anisotropy vs (2) chain interdiffusion. However, the tensile strength increases during this period, strongly suggesting normal interdiffusion. Thus, within experimental error, the relaxation of anisotropy and molecular interdiffusion are thought to be about equal in magnitude, but opposite in effect.

Surprisingly, tensile strength was fully developed at a penetration depth of 28 Å. Correcting for the molecular weight differences between the deuterated and protonated polystyrene chains yields a penetration depth of 30–35 Å. The correction was based on well-known relationships which state that the diffusion coefficient is inversely proportional to the squared molecular weight and that the distance a molecule travels is proportional to the square root of time. Therefore, for the current system, the minimum penetration depth for full tensile strength is comparable to the radius of gyration of the critical entanglement molecular weight, which is approximately 32 000 g/mol. It should be pointed out that in another experiment using polystyrene latex particles of M_w = 1 960 000, annealed at 152 °C, a minimum penetration depth of 40–50 Å was required to obtain full tensile strength.[42]

The previous low molecular weight polystyrene[22] developed full tensile strength at the penetration depth comparable to the radius of gyration of whole chains. (Then, half of the chain is on each side of the original

Table IV
Comparison of High and Low Molecular Weight Data[a]

	$M_w \simeq 2\,000\,000$		$M_w = 250\,000$	
annealing time	d, Å	TS × 10^5, N/m²	d, Å	TS × 10^5, N/m²
sintered		34		41
5 min	15	52	24	49
15 min	15	64	36	149
30 min	15	120	47	225
1 h	19	226	79	249
2 h	28	389	113	315
4 h	32	389	128	328
8 h	35	371	N/A	288
19 h	43	345	N/A	276
48 h	55	366	N/A	312

[a] d = depth of penetration, TS = tensile strength, N/A = not available.

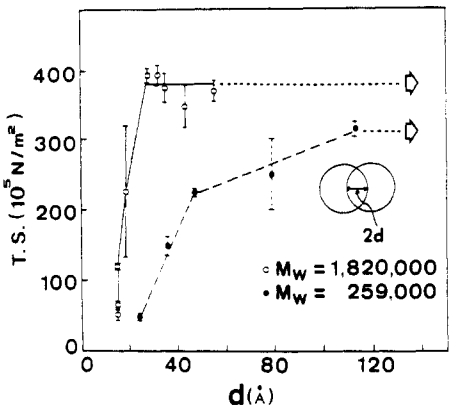

Figure 3. Plot showing that the tensile strength for the high molecular weight polystyrene increases faster, yielding the higher ultimate tensile strength; the low molecular weight data are from the previous paper.[22]

interface.) For convenience, the low and high molecular weight data are compared in Table IV. Figure 3 illustrates the tensile strength buildup behavior as a function of the average depth of penetration, d, for both molecular weight polystyrenes. It is noted that the ultimate tensile strength of the high molecular weight polystyrene is higher than that of the low molecular weight counterpart. Interestingly, it is observed that the high molecular weight species shows the faster rate of increase in tensile strength.

Another surprising feature of the high molecular weight data is the fact that full tensile strength was achieved at almost the same time as that for the low molecular weight polystyrene at the same annealing temperature, 144 °C. The time dependency of the tensile strength buildup for the high molecular weight polystyrene is shown in Figure 4. While this figure assumes that the tensile strength increases with time to the one-fourth power, it is instructive to plot the critical portions of the data on a log–log basis (Figure 5). The low molecular weight sample yields a slope of 0.27, well within the experimental error of 0.25. However, the high molecular weight sample yields a much higher slope, 0.69. This anomaly will be discussed below.

The above-mentioned theories predict that the interpenetration depth, d, will increase with the square root of annealing time. As illustrated in Figure 6, reasonably straight lines are obtained for both materials, albeit with quite large differences in slopes. Extrapolation of the data to zero time yields an apparent initial interpenetration of about 10 Å. This may be the combined results of initial sintering, plus annealing as the samples were heated to temperatures, before the clock was started. Again, it is instructive to plot the data on a log–log basis (Figure 7). While the low molecular weight data yield a slope of 0.49,

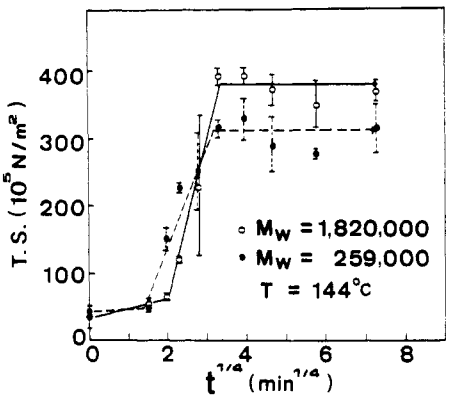

Figure 4. Plot showing that tensile strength increases with time to the one-fourth power, after an apparent induction period. Full tensile strength for both molecular weight samples is developed in the same time frame: the low molecular weight data are from the previous paper.[22] Error bars are indicated.

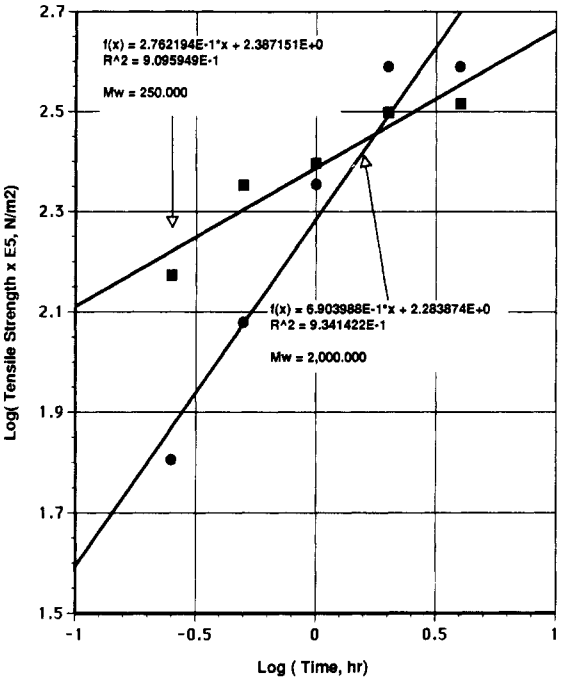

Figure 5. log–log plot showing the increase in tensile strength with time.

with 97% of the variability explained by the linear model again within the experimental error of 0.50. However, the high molecular weight data again show an anomaly, with a slope of only 0.38, significantly lower. This, too, will be discussed below.

Discussion

Location of Polymer Chain Ends. The polymerization reaction produces a polymer molecule with two sulfate ion chain ends.[43] These sulfate ion chain ends are predominantly anchored at the latex particle–water interface because of the strong hydrophilicity of the ionic end groups.

It must be pointed out that the relaxed chain dimension of the present high molecular weight polystyrene is much larger than the particle diameter. Accordingly, it would be reasonable to assume that the present high molecular weight polystyrene has both chain ends on the particle surface. However, the situation for low molecular weight polystyrene is somewhat different because chain-transfer agents were used in its polymerization. Comparing the molecular weights between the low and high molecular

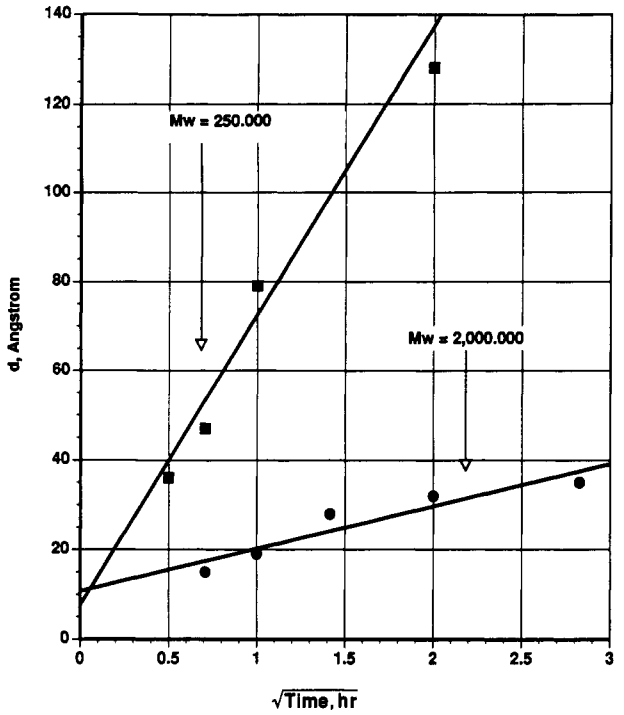

Figure 6. Plot showing that penetration distance increases much slower for the high molecular weight specimen than for the low molecular weight sample.

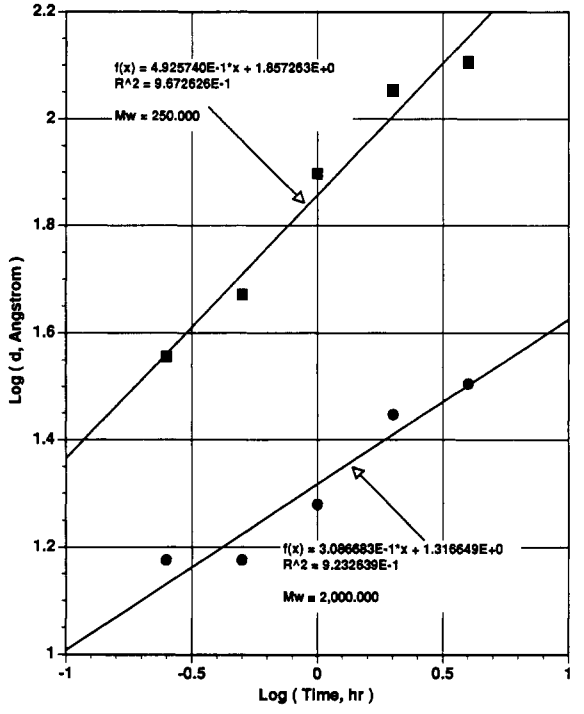

Figure 7. Wool theory predicts a slope of 0.5 for this log d–log t plot.

weight samples containing the same amount of the sulfate initiators, a large fraction of low molecular weight polystyrene chains do not have ionic end groups. Therefore, the chain ends of the low molecular weight polystyrene sample are relatively free to position themselves inside latex particles.

As such, there is a difference in the location of chain ends inside latex particles between the low and high molecular weight polystyrene latex particles, at least on a relative basis. With the qualitative models shown in Figure 8, the effect of chain end location on the minimum

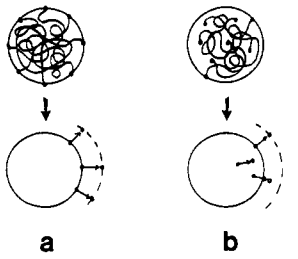

Figure 8. Qualitative models explaining the role of chain ends in latex film formation: (a) case where all chain ends are on the particle surface; (b) case where chain ends are randomly distributed.

penetration depth for the full tensile strength is discussed. In Figure 8, diagrams a and b represent the same molecular weight latex particles with different spatial distributions of chain ends.

As already pointed out by de Gennes,[11,28] chain ends can determine the direction toward which polymer chains diffuse whereas the impingement of any other portion of chains is unlikely to happen. Then, let us take a look at the displacement of the chain ends in each case after a certain period of annealing. As shown in Figure 8, polymer chains with their ends on the particle surface more effectively diffuse into neighboring particles, contributing more to the rapid formation of new entanglements. However, those with their ends inside latex particles need to diffuse a longer distance before they can contribute to interparticle entanglement formation depending on the distance of the chain ends from the surface. Therefore, polymer chain ends with a random distance from the particle surface must diffuse further to achieve one entanglement per chain in the other particle, necessary for the development of full tensile strength.

The above interpretation inspires a hypothesis that the minimum penetration depth for full material strength development in general interface healing need not depend primarily on the polymer chain molecular weight but also on the spatial distribution of chain ends near the interface.

To verify the above hypothesis, the present results are compared with the results published so far. Table V summarizes the experimental findings in polymer interface healing to date. It demonstrates a trend that the higher the population of chain ends at the interface is, the smaller is the minimum penetration depth for full material strength, being substantially independent of the molecular weight of polymer chains. This strongly supports the supposition that the spatial distribution of chain ends near the interface, not the molecular weight, controls the minimum penetration depth of polymer chains for the development of full material strength in polymer interface healing.

If we presume that for full mechanical strength one entanglement per diffusing molecule is needed beyond the interface, then in the limit two cases may be distinguished: the distance distribution of chain ends from the interface is narrow and most of the chain ends are at the interface, and the distance distribution is broad and most of the chain ends are away from the interface.

Based on the minor chain reptation model[5] for film formation the mechanical strength will be fully developed in the first case when each chain end has diffused the equivalent distance of the critical entanglement R_g and, in the second limiting case, when the diffusing molecules have achieved maximum overlap at the interface, which occurs at the equivalent distance of one R_g of the chains.

One-Fourth or One-Half Power Time Dependence? In the theory section, the essential features of the various

Table V
Summary of the Minimum Penetration Depth for Full Material Strength Reported in the Interface Healing of Polymers

interface healing	ref	materials	strength test	min depth of penetration, Å	population of chain ends at interface
crack healing	15	PMMA (M_w = 120 000)	compact tension	20–30 (calcd)	high
latex film formation	3	PS (M_w = 5.8 × 10^6)	indentation toughness	50–60 (obsd)	high
latex film formation	a	PS (M_w ≃ 2.0 × 10^6)	tensile strength	30–35 (obsd)	high
latex film formation	22	PS (M_w = 250 000)	tensile strength	110–120 (obsd)	intermediate to low
polymer welding	18	PS (M_w = 262 000)	lap shear strength	170 (calcd)	low

[a] Current work.

models of time and molecular weight dependence on polymer surface healing were described. In order to discuss our results, however, some of the finer points in the theories must be brought out.

The Prager and Tirrell model[7-9,12] assumed that mechanical property recovery depends on the total molecular crossing density at the interface. They calculated the crossing density for two cases: equilibrium or uniform chain end distributions throughout the bulk, and excess chain ends at the initial interfaces. These two cases yielded a one-half and one-fourth power dependence on time, respectively. The fracture stress dependence on time is intimately connected to the relationship used between crossing density and stress. According to the Griffith theory of fracture, crack initiation occurs when the stored elastic energy equals the energy required for the generation of the new crack surface. New surface alone accounted for only a tiny fraction of the work required. Then, in a virgin linearly elastic polymer, the energy for the fresh crack surface generation was assumed to be proportional to the crossing density. Since the elastic energy release is related to the square of the applied stress, the fracture stress becomes dependent on the one-half power of the crossing density. This then yields a fracture stress dependence on the power time of one-fourth and one-eighth. Prager and Tirrell argued, however, that in crack healing, which is analogous to the healing of latex particle interfaces, the stored elastic energy is different from the virgin polymer case. Consideration that at small healing times the stored energy is concentrated in the weakened regions leads to a more reasonable assumption, when relating the fracture stress to the crossing density, rather than the crossing density to the one-half power. Thus, Prager and Tirrell predict the fracture stress development with time to be one-fourth power at early times of healing, when chain ends residing on the initial surface cross the interface, which dependence changes over the one-half power later on, when chains from the bulk start to cross the interface.

The Kim and Wool model,[4,5] in contrast, is based on the assumption that the fracture stress depends on the interpenetration distance. With the chain end distribution taken as uniform through the bulk, they found that the fracture stress is dependent on time to the one-fourth power.

In Figure 5 the low and high molecular weight sample fracture stress dependence on annealing time is shown. The one-fourth power dependence for the low molecular weight sample holds for the entire range of healing. No change to one-half power dependence is observed. For the high molecular weight case, however, a one-half power dependence would be a better fit than one-fourth. This interpretation, too, has many problems. First, one must assume that the chain ends were uniformly distributed, which is contrary to the current thinking for the high molecular weight polymer with ionic ends.

Table VI
Effect of the Dimensional Ratio on the Chain Conformation Inside Latex Particles

dimensional param	high mol wt (M_w ≃ 2 000 000)	low mol wt (M_w = 250 000)
end-to-end distance ($\bar{r}$, Å)	953	336
particle size (D_p, Å)	450	464
chain conformation	constrained	relaxed

In this analysis, one must further consider the possible effect of the broad molecular weight distribution. The high molecular weight fraction polymer chain ends most likely reside on the particle surface and the lower molecular weight fraction chain ends may well be uniformly distributed. The faster molecular process is most likely to control the healing process at the interface. The time dependence of the surface end group contribution may be thus masked by the low molecular weight chain end contribution. The ultimate strength, however, may reflect the presence of the high molecular weight fraction, the ends of which had to diffuse a shorter distance than those ends in the bulk.

Dimensionless Ratio of Polymer Chain R_g to Latex Radius. Returning to latex film formation problems, the present high molecular weight polystyrene latexes carry an important characteristic in terms of the dimension of polymer chains inside latex particles relative to the particle radius. For polystyrene random coils, it is known that in the relaxed state[44,45] the radius of gyration, R_g, is related to the weight-average molecular weight, M_w, by

$$R_g = 0.275 M_w^{1/2} \quad (12)$$

and the end-to-end distance, $\bar{r}$, is obtained by the relationship

$$\bar{r}^2 = 6R_g^2 \quad (13)$$

In Table VI the theoretical end-to-end distances and the latex particle diameters determined by SANS are listed for the high and low molecular weight latex particles. As previously reported by Linné et al.,[3] the high molecular weight polystyrene chains are highly constrained in small latex particles whereas the low molecular weight polystyrene chains are likely to have a relaxed chain conformation due to the small size of the chains relative to the particles; see Figure 9.

It is evident that the constrained nature of the high molecular weight chains will provide an additional driving force for diffusion until the chains are fully relaxed based on entropic considerations. In this sense, it is interesting to perceive that the high molecular weight chains can

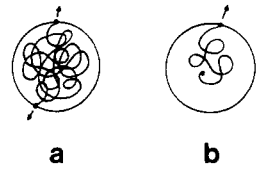

Figure 9. Model showing conformational entropic effect, which provides additional driving for diffusion: (a) high molecular weight case; (b) low molecular weight case.

diffuse out into two directions simultaneously (see Figure 9), whereas the low molecular weight ones cannot.

On the basis of Binder's theory[37] and the Summerfield–Ullman theory[39] discussed earlier in the data analysis section, SANS data for the high molecular weight polystyrene samples were analyzed to give a diffusion coefficient of 3.7×10^{-17} cm^2/s at $K = 0.0055$ Å^{-1} and 144 °C. Under the same conditions, that of the low molecular weight samples was reported to be 4.0×10^{-16} cm^2/s.[22] Theoretically, the diffusion coefficient is inversely proportional to squared molecular weight. This means that the ratio of the diffusion coefficients of the high to the low molecular weight polystyrenes should be 0.014 based on M_w.[46] However, the observed ratio is 0.093, much higher than theoretical, which supports the presence of an additional driving force for diffusion in the high molecular weight system.

Phase Separation Considerations. Noting the works of Bates et al.,[47-51] we take under consideration the problem of whether the current system of high molecular weight protonated and deuterated polystyrenes was or was not miscible. The Flory–Huggins free energy of mixing (ΔF_m) expression is based on the degree of polymerization, N, of the polymers under consideration. In a monodisperse system the equation can be written[52,53] for deuterated (D) and protonated (H) polystyrene mixtures:

$$\frac{\Delta F_m}{kT} = \frac{\phi_D}{N_D} \ln \phi_D + \frac{\phi_H}{N_H} \ln \phi_H + \phi_D \phi_H \chi \qquad (14)$$

where k represents the Boltzmann constant, T stands for temperature, ϕ is volume fraction, and χ is the Flory–Huggins interaction parameter. The interpretation of N for a heterodisperse system must be discussed. According to Flory,[52] where the polymers are confined as a whole to one phase, the chemical potential averaged over all polymer species is required. Under these conditions, eq 15 should be used with N replaced by its number-averaged quantity, N_n.[52,54]

To calculate the phase diagram, we need to determine the temperature dependence of χ in eq 15. This has been measured by Bates[47,48] for three different molecular weights for 50/50 protonated/deuterated systems. Its experimentally determined temperature dependence[48] is

$$\chi = 0.2/T - 2.9 \times 10^{-4} \qquad (15)$$

From eqs 15 and 16, the phase diagrams illustrated in Figure 10 were calculated. For illustration purposes, several symmetrical number-average degrees of polymerization were assumed, since none of these important plots have yet been published. The assumption made in these calculations is that χ is independent of composition. Note that the present case is nearly symmetrical for molecular weights but has a 6/94 deuterated/protonated composition ratio. According to Figure 10, the number-average values of N calculated from Table II are one phased.

Another important point for establishing the miscibility of the two polymers related to the determination of the molecular weight of the deuterated species at long diffusion times. For low molecular weight polystyrene, as reported in the previous paper,[22] we obtained the same molecular weight, 250 000 g/mol, by SANS and by GPC, after 48 h of annealing at 144 °C. It was of interest to observe whether a similar result could be extracted from the present high molecular weight data. Briefly, the results were as follows.

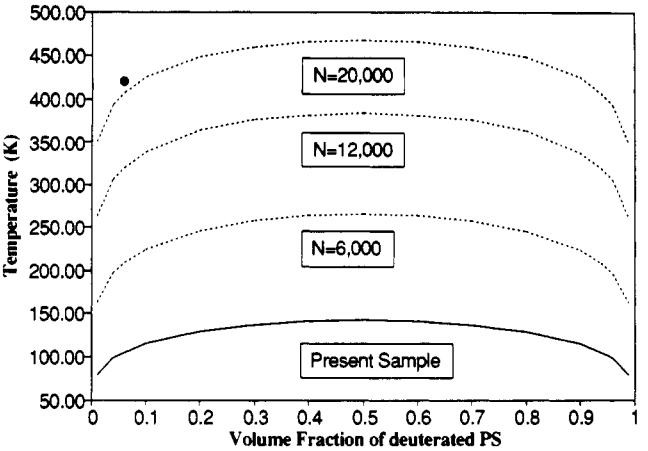

Figure 10. Flory–Huggins phase diagram for mixtures of deuterated and protonated polystyrene: the present experimental conditions (●) are located in one phase region.

A Guinier analysis of the 48-h annealing data was carried out to extrapolate the scattering intensities to zero angle. The data, transformed into absolute scattering intensities, gave $M_w = 6.3 \times 10^6$, or an average segregation of three polystyrene chains remaining. In data to be published, the experiment on a similar high molecular weight polystyrene ($M_w = 2.08 \times 10^6$) was continued for 7 days at 152 °C.[42] After that annealing time, the weight-average molecular weight determined by SANS was determined to be 2.9×10^6, almost totally interdiffused.

While the evidence is significant that the protonated and deuterated high molecular weight polystyrenes used are miscible, there is evidence that the experiment may have been affected by "thermodynamic slowdown".[55] This means that although the protonated and deuterated portions are actually mutually miscible, their interdiffusion rate is slowed down by the relatively poor thermodynamics of mixing. This is exemplified by the nonclassical results depicted in Figures 6 and 7. It may also explain why the apparent interdiffusion distance measured by SANS was only 35 Å when full tensile strength was achieved.

While it is unknown exactly how much the "thermodynamic slowdown", if any, affected the high molecular weight experiments, it is probable that we have measured the minimum interdiffusion distance and that the actual value is probably somewhat higher.

In the area of latex film formation, particle size, molecular weight, and composition have been of major concerns. Additionally, we propose two new critical parameters in the process of film formation from latexes: the location of chain ends and the dimensional ratio of polymer chains to the particle size.

From an engineering point of view, it must be noted that high tensile strengths will be most rapidly achieved when (a) the latexes are small, (b) the molecular weights are high, and (c) the chain ends are on the surface of the latexes. These considerations may shed light on the latex film formation from both theoretical and practical viewpoints.

Conclusions

SANS studies on polymer chain interdiffusion during film formation from polystyrene latex particles have elucidated a number of fundamental aspects of film formation as well as general polymer interface healing. The minimum penetration depth for high molecular weight polystyrene full tensile strength was found to be at least 30–35 Å, comparable to the radius of gyration of the critical entanglement molecular weight for polystyrene.

Comparing the present results with those reported previously has led to the supposition that the minimum penetration depth for full mechanical strength in the interface healing such as crack healing, film formation, and polymer welding may be partly controlled by the spatial distribution of chain ends near the interface as well as by molecular weight. Two critical parameters in the interdiffusion of film formation from latex particles are proposed: the location of chain ends and the dimensionless ratio of the polymer chains' radii of gyration to the latex particle's radius.

Acknowledgment. We thank the National Science Foundation for support through Grant No. CBT-8820705. The SANS experiments were performed at the National Institute of Standards and Technology (NIST) and Los Alamos Neutron Scattering Center (LANSCE). We thank Dr. Philip A. Seeger and Dr. Rex P. Hjelm, Jr., for their many helpful discussions and assistance with the SANS experiment at LANSCE.

References and Notes

(1) Hahn, K.; Ley, G.; Schuller, H.; Oberthür, R. *Colloid Polym. Sci.* **1986**, *264*, 1092.
(2) Hahn, K.; Ley, G.; Oberthür, R. *Colloid Polym. Sci.* **1988**, *266*, 631.
(3) Linné, M. A.; Klein, A.; Miller, G. A.; Sperling, L. H. *J. Macromol. Sci., Phys.* **1988**, *B27* (2&3), 217.
(4) Wool, R. P.; O'Conner, K. M. *J. Appl. Phys.* **1981**, *52*, 5953.
(5) Kim, Y. H.; Wool, R. P. *Macromolecules* **1983**, *16*, 1115.
(6) Adolf, D.; Tirrell, M.; Prager, S. *J. Polym. Sci., Polym. Phys. Ed.* **1985**, *23*, 413.
(7) Prager, S.; Tirrell, M. *J. Chem. Phys.* **1981**, *75*, 5194.
(8) Prager, S.; Adolf, D.; Tirrell, M. *J. Chem. Phys.* **1986**, *84*, 5152.
(9) Prager, S.; Adolf, D.; Tirrell, M. *J. Chem. Phys.* **1983**, *78*, 7015.
(10) Jud, K.; Kausch, H. H.; Williams, J. G. *J. Mater. Sci.* **1981**, *16*, 204.
(11) de Gennes, P.-G. *J. Chem. Phys.* **1971**, *55*, 572.
(12) Tirrell, M.; Adolf, D.; Prager, S. *Springer-Verlag Lect. Notes Appl. Math.* **1984**, *1063*, 37.
(13) Zhang, H.; Wool, R. P. *Macromolecules* **1989**, *22*, 3018.
(14) Voyutskii, S. S. In *Autohesion and Adhesion of High Polymers*; Interscience: New York, 1963.
(15) Wool, R. P.; Yuan, B. L.; McGarel, O. J. *Polym. Eng. Sci.* **1989**, *29*, 1341.
(16) Kausch, H. H.; Petrovska, D.; Landel, R. F.; Monnerie, L. *Polym. Eng. Sci.* **1987**, *27*, 149.
(17) McGarel, O. J.; Wool, R. P. *J. Polym. Sci., Polym. Phys. Ed.* **1987**, *25*, 2541.
(18) Kline, D. B.; Wool, R. P. *Polym. Eng. Sci.* **1988**, *28*, 52.
(19) Nguyen, T. Q.; Kausch, H. H.; Jud, K.; Dettenmaier, M. *Polymer* **1982**, *23*, 1305.
(20) Roland, C. M.; Bohm, G. G. A. *Macromolecules* **1985**, *18*, 1310.
(21) Brown, H. R.; Yang, A. C. M.; Russell, T. P.; Volksen, W.; Kramer, E. J. *Polymer* **1988**, *29*, 1807.
(22) Yoo, J. N.; Sperling, L. H.; Glinka, C. J.; Klein, A. *Macromolecules* **1990**, *23*, 3962.
(23) Yoo, J. N.; Sperling, L. H.; Klein, A. *Polym. Mater. Sci. Eng. (Prepr.)* **1989**, *61*, 738.
(24) Tirrell, M. *Rubber Chem. Technol.* **1984**, *57*, 523.
(25) Mills, P. J.; Green, P. F.; Palmstrom, C. J.; Mayer, J. W.; Kramer, E. J. *Appl. Phys. Lett.* **1984**, *45*, 957.
(26) Green, P. F.; Kramer, E. J. *Macromolecules* **1986**, *19*, 1108.
(27) Green, P. F.; Mills, P. J.; Kramer, E. J. *Polymer* **1986**, *27*, 1063.
(28) de Gennes, P.-G. *C. R. Acad. Sci. Paris* **1980**, *B291*, 219.
(29) van del Hul, H. J.; Vanderhoff, J. W. *Br. Polym. J.* **1970**, *2*, 121.
(30) Vanderhoff, J. W. *Pure Appl. Chem.* **1980**, *52*, 1263.
(31) Vanderhoff, J. W.; van del Hul, H. J. In *Polymer Colloids*; Fitch, R. M., Ed.; Plenum: New York, 1971.
(32) Vanderhoff, J. W.; van del Hul, H. J. *J. Colloid Interface Sci.* **1968**, *28*, 36.
(33) Jayasuriya, R. M.; El-Aasser, M. S.; Vanderhoff, J. W.; Yue, H. J. *J. Polym. Sci., Polym. Chem. Ed.* **1985**, *23*, 2819.
(34) Glinka, C. J.; Rowe, J. M.; LaRock, J. G. *J. Appl. Crystallogr.* **1986**, *19*, 427.
(35) Hjelm, R. P. *J. Appl. Crystallogr.* **1988**, *21*, 618.
(36) Guinier, A.; Fournet, G. In *Small Angle Scattering of X-rays*; John Wiley & Sons: New York, 1955.
(37) Binder, K. *J. Chem. Phys.* **1983**, *79*, 6387.
(38) Cook, H. *Acta. Metall.* **1970**, *18*, 297.
(39) Summerfield, G. C.; Ullman, R. *Macromolecules* **1988**, *21*, 2643.
(40) (a) Anderson, J. E.; Jou, J. H. *Macromolecules* **1987**, *20*, 1544. (b) Jou, J. H. Ph.D. Dissertation, The University of Michigan, 1986.
(41) Kramer, E. J.; Green, P. F.; Palmstrom, C. J. *Polymer* **1984**, *25*, 473.
(42) Yoo, J. N. Ph.D. Dissertation, Lehigh University, 1990.
(43) Tedder, J. M. In *Reactivity, Mechanism and Structure in Polymer Chemistry*; Jenkins, A. D., Ledwith, A., Eds.; Wiley-Interscience: New York, 1974.
(44) Cotton, P. J.; Decker, D.; Benoit, H.; Farnoux, B.; Higgins, J.; Jannink, G.; Ober, R.; Picot, C.; des Cloizeaux, J. *Macromolecules* **1974**, *7*, 863.
(45) Wignall, G. D.; Ballard, D. G.; Schelten, J. J. *Eur. Polym. J.* **1974**, *10*, 861.
(46) Mills, P. J.; Green, P. F.; Palmstrom, C. J.; Mayer, J. W.; Kramer, E. J. *J. Polym. Sci., Polym. Phys. Ed.* **1986**, *24*, 1.
(47) Bates, F. S.; Wignall, G. D. *Macromolecules* **1986**, *19*, 932.
(48) Bates, F. S.; Wignall, G. D. *Phys. Rev. Lett.* **1986**, *57*, 1429.
(49) Bates, F. S.; Dierker, S. B.; Wignall, G. D. *Macromolecules* **1986**, *19*, 1938.
(50) Bates, F. S. *J. Appl. Crystallogr.* **1988**, *21*, 681.
(51) Bates, F. S.; Wiltzius, P. J. *Chem. Phys.* **1989**, *91*, 3258.
(52) Flory, P. J. In *Principles of Polymer Chemistry*; Cornell University Press: Ithaca, NY, 1953.
(53) de Gennes, P. G. In *Scaling Concepts in Polymer Physics*; Cornell University Press: Ithaca, NY, 1979.
(54) Saeki, S.; Cowie, J. M. G.; McEwen, I. J. *Polymer* **1983**, *24*, 60.
(55) Green, P. F.; Doyle, B. L. In *New Characterization Techniques for Thin Polymer Films*; Tong, H. M., Nguyen, L. T., Eds.; Wiley-Interscience: New York, 1990.